Biosensors and Bioelectronics 121 (2018) 174–182

Contents lists available at ScienceDirect

Biosensors and Bioelectronics

journal homepage: www.elsevier.com/locate/bios

Tracking tonic dopamine levels *in vivo* using multiple cyclic square wave voltammetry

Yoonbae Oh[a], Michael L. Heien[b], Cheonho Park[c], Yu Min Kang[c], Jaekyung Kim[c], Suelen Lucio Boschen[a], Hojin Shin[c], Hyun U. Cho[c], Charles D. Blaha[a], Kevin E. Bennet[a,d], Han Kyu Lee[e], Sung Jun Jung[e], In Young Kim[c], Kendall H. Lee[a,f,*,1], Dong Pyo Jang[c,**,1]

[a] Department of Neurologic Surgery, Mayo Clinic, Rochester, MN 55905, United States
[b] Department of Chemistry and Biochemistry, University of Arizona, Tucson, AZ 85721, United States
[c] Department of Biomedical Engineering, Hanyang University, Seoul 04763, Republic of Korea
[d] Division of Engineering, Mayo Clinic, Rochester, MN 55901, United States
[e] Department of Biomedical Science, Graduate School of Biomedical Science and Engineering, Hanyang University, Seoul 04763, Republic of Korea
[f] Department of Physiology and Biomedical Engineering, Mayo Clinic, Rochester, MN 55905, United States

ARTICLE INFO

Keywords:
Electrochemistry
Dopamine
Carbon-fiber microelectrodes
Striatum
Rat

ABSTRACT

For over two decades, fast-scan cyclic voltammetry (FSCV) has served as a reliable analytical method for monitoring dopamine release in near real-time *in vivo*. However, contemporary FSCV techniques have been limited to measure only rapid (on the order of seconds, *i.e.* phasic) changes in dopamine release evoked by either electrical stimulation or elicited by presentation of behaviorally salient stimuli, and not slower changes in the tonic extracellular levels of dopamine (*i.e.* basal concentrations). This is because FSCV is inherently a differential method that requires subtraction of prestimulation tonic levels of dopamine to measure phasic changes relative to a zeroed baseline. Here, we describe the development and application of a novel voltammetric technique, multiple cyclic square wave voltammetry (M-CSWV), for analytical quantification of tonic dopamine concentrations *in vivo* with relatively high temporal resolution (10 s). M-CSWV enriches the electrochemical information by generating two dimensional voltammograms which enable high sensitivity (limit of detection, 0.17 nM) and selectivity against ascorbic acid, and 3,4-dihydroxyphenylacetic acid (DOPAC), including changes in pH. Using M-CSWV, a tonic dopamine concentration of 120 ± 18 nM (n = 7 rats, ± SEM) was determined in the striatum of urethane anethetized rats. Pharmacological treatments to elevate dopamine by selectively inhibiting dopamine reuptake and to reduce DOPAC by inhibition of monoamine oxidase supported the selective detection of dopamine *in vivo*. Overall, M-CSWV offers a novel voltammetric technique to quantify levels and monitor changes in tonic dopamine concentrations in the brain to further our understanding of the role of dopamine in normal behavior and neuropsychiatric disorders.

1. Introduction

Dopamine has a variety of roles in the brain, and is involved in learning and memory (Jay, 2003), motivation and emotional behaviors (LeDoux, 2012), and action-selection (Balleine et al., 2007). Dysfunction in dopamine signaling is thus implicated in several neurologic and psychiatric diseases, including Parkinson's disease, drug addiction, depression, and schizophrenia (Grace, 2016; Hyman and Malenka, 2001). Dopamine neurons exhibit two distinct patterns of spike firing: tonic activity and phasic burst activity (Grace, 2016). Phasic activity causes a transient and robust release of dopamine that serves as a learning signal for neural plasticity. Tonic activity refers to spontaneous and continuous dopamine release driven by pacemaker-like firing of dopamine neurons, providing a tonic extracellular level of dopamine (*i.e.* basal concentration) in the striatum required to modulate behavioral flexibility (Goto et al., 2007). In addition, tonic dopamine concentrations are known to be modulated by the escape of dopamine from the extrasynaptic space (Floresco et al., 2003), inhibition by GABAergic interneurons (Grace and Bunney, 1984), receptor occupancy, dopamine transporter function, and synaptic plasticity (Grace, 2000; Schultz,

* Correspondence to: Mayo Clinic, 200 First Street SW, Rochester, MN 55905, USA.
** Corresponding author.
E-mail address: dongpjang@hanyang.ac.kr (D.P. Jang).
[1] KHL and DPJ supervised all aspects of this work equally.

https://doi.org/10.1016/j.bios.2018.08.034
Received 11 June 2018; Received in revised form 13 August 2018; Accepted 16 August 2018
Available online 20 August 2018

2007).

Tonic concentrations of dopamine in the brain have been typically quantified in the low nM range using microdialysis combined with high-performance liquid chromatography (Gu et al., 2015), whereas fast-scan cyclic voltammetry (FSCV) has been used for monitoring relatively fast transients of phasic dopamine release *in vivo* (Heien et al., 2005). Despite superior selectivity and sub-nanomolar limit of detection provided by microdialysis, it has several drawbacks based on the dialysis probe dimensions that include variable physico-chemical characteristics, tissue damage, and relatively low spatiotemporal resolution (Stenken, 1999; Justice, 1993). In contrast, FSCV, in combination with carbon-fiber microelectrodes (CFM), provides superior biocompatibility, rapid response time, and high spatiotemporal resolution also based on the minimal dimensions of the CFM (Huffman and Venton, 2009; Robinson et al., 2003). However, conventional FSCV techniques are unable to measure tonic dopamine levels because background subtraction of large background capacitive currents present in the raw voltammogram is required to quantify faradaic dopamine redox currents (Howell et al., 1986).

Recently, modified FSCV techniques have been developed that enable measurment of slow changes in tonic dopamine levels *in vivo* (Oh et al., 2016; Atcherley et al., 2015; Atcherley et al., 2013; Abdalla et al., 2017; Burrell et al., 2015). These techniques use differential methods with multiple waveforms and take advantage of the adsorption properties of amine neurotransmitters to the CFM surface. In addition, a microfabricated sensor has been developed to perturb the local dopamine concentration, thus allowing the sensor to estimate *in vitro* tonic dopamine concentrations (Dengler and McCarty, 2013). Essentially, measuring tonic dopamine concentrations using voltammetric techniques are a matter of isolation or elimination of capacitive background current from faradaic current of electroactive species without using conventional background subtraction methods. A number of studies have modelled the characteristics of capacitive background currents at recording electrodes in aqueous solutions and *in vivo* (Dengler and McCarty, 2013). However, these models have not been entirely successful in eliminating background currents to quantify tonic dopamine levels.

Here we introduce a new technique termed multiple cyclic square wave voltammetry (M-CSWV) for quantifying tonic dopamine concentrations *in vivo*. The technique uses cyclic square wave voltammetric waveforms in conjunction with a delayed holding potential period to control dopamine adsorption to the CFM surface. Unlike conventional analysis of square wave voltammetric data (Osteryoung and Osteryoung, 1985; Helfrick and Bottomley, 2009), background currents recorded at all waveform points were sampled and used to detect and quantify tonic dopamine concentrations. Dynamic background subtraction (Oh et al., 2016) and capacitive background current simulation were used to eliminate large capacitive background current, allowing tonic dopamine concentrations to be measured. The cyclic square waveform (CSW) consisted of a large–amplitude square wave modulation on top of a symmetric staircase waveform. Because of the uniqueness of the waveform, the voltammetric outcome of M-CSWV provides a wealth of electrochemical information beyond that provided by conventional FSCV. Specially, multiple redox reactions of dopamine occur within a scan that enables the technique to generate a two-dimensional voltammogram. Parameters of M-CSWV were optimized *in vitro* to detect dopamine at ten-second intervals. It was shown to be highly sensitive (limit-of-detection < 1 nM, 3 times the RMS noise) and selective against 3,4-dihydroxyphenylacetic acid (DOPAC) and ascorbic acid (AA). In addition, we demonstrated its *in vivo* analytical capability for measuring tonic dopamine concentrations in the striatum of anesthetized rats (120 ± 18 nM, n = 7 rats, ± SEM) with pharmacological confirmation.

2. Materials and methods

2.1. Data collection and analysis

M-CSWV was performed using a commercial electronic interface (NI USB-6363, National Instruments) with a base-station PC and software written in-house using LabVIEW 2016 (National Instruments, Austin, TX). Data, in the form of a sequence of unsigned 2-byte integers, were saved to the base-station computer and processed by MATLAB (MathWork Inc., Natick, MA). The processing includes temporal averaging, filtering, and simulating background currents. GraphPad Prism 5 (GraphPad Software, San Diego, CA) was used to generate figures and perform statistics (one-way, two-way ANOVA with multiple comparisons, *etc.)*. All data are presented as mean ± standard error of the mean (SEM) values for n number of electrodes or rats.

2.2. Analysis of dopamine response to M-CSWV

A “dopamine-kernel” method was developed to extract the dopamine-featured response from M-CSWV. To make a dopamine-kernel, we used the dopamine oxidative response of M-CSWV and applied a threshold algorithm where signals greater than 60% of the maximum oxidation current amplitude are given a value of one in the dopamine-kernel. A dopamine-kernel, K, was then applied to the dopamine response of M-CSWV, by multiplying each element of dopamine-kernel, k_{ij}, to a corresponding element of the M-CSWV response, vij.

$$K \odot V = k_{ij} \times v_{ij} \mid \; i \in [1, \ldots, n] \text{ and } j \in [1, \ldots, m]$$

Where i and j are the index of row and column respectively, and K and V have the same matrix size (n x m). For each CFM, the dopamine-kernel was determined from *in vitro* dopamine experiments and applied to analyse *in vivo* data.

2.3. Carbon-fiber microelectrodes (CFMs)

Electrodes were fabricated as previously described (Oh et al., 2016). AS4 carbon fiber (Hexel, Stamford, CT) was used for all experiments. The exposed carbon fiber was trimmed to approximately 50 μm in length, then PEDOT: nafion coating was applied onto the exposed carbon fiber for all electrodes (Vreeland et al., 2015). The microelectrodes were dried overnight at room temperature. Additional details are available in the Supporting Information.

2.4. Chemicals

Dopamine HCl, DOPAC, and AA were dissolved in distilled water at a stock concentration of 1 mM, 10 mM, and 100 mM, respectively, and preserved in 0.1 M perchloric acid. Samples from the stock solutions were diluted with TRIS buffer (15 mM tris, 3.25 mM KCl, 140 mM NaCl, 1.2 mM $CaCl_2$, 1.25 mM NaH_2PO_4, 1.2 mM $MgCl_2$, and 2.0 mM Na_2SO_4, with the pH adjusted to 7.4) for desired concentration. All chemicals, including nomifensine maleate salt and pargyline HCl, were purchased from Sigma-Aldrich (St. Louis, MO).

2.5. Preparation of brain slices for Ca^{2+} imaging

Mouse striatum slice preparation and Ca^{2+} imaging experimental procedures were performed according to NIH guidelines and approved by the Hanyang University Institutional Animal Care and Use Committee. Additional details regarding the Ca^{2+} imaging protocol are described in the Supporting Information.

2.6. In vivo experiments

Adult male Sprague Dawley rats weighing 250–350 g were used for the *in vivo* experiments in these studies (n = 5, each group). NIH

guidelines were followed for all animal care, and the Mayo Clinic Institutional Animal Care and Use Committee approved the experimental procedures. WINCS Harmoni was used to perform FSCV and electrical stimulation to identify dopamine releasing sites in the dorsomedial striatum (Lee et al., 2017). Once an optimal CFM recording site was identified, the device was changed to the M-CSWV recording system for tonic dopamine concentration recording. Additional details regarding the *in vivo* experimental protocol are described in the Supporting Information.

3. Results and discussion

3.1. Multiple cyclic square wave voltammetry (M-CSWV)

Conventional FSCV with background subtraction techniques can readily measure phasic changes in dopamine release, but cannot measure tonic concentrations of dopamine because FSCV requires background subtraction. Recently, modified FSCV techniques have been developed to measure dopamine tonic levels *in vivo* (Oh et al., 2016; Atcherley et al., 2015, 2013; Abdalla et al., 2017). We used the same principles reported in previous studies, namely the adsorption characteristics of dopamine on the CFM surface, to conduct M-CSWV. In contrast to these previous methods, M-CSWV provides significantly higher temporal resolution (10 s) and additional dimensional analysis in the voltammogram by using a modified form of cyclic square wave voltammetry.

Fig. 1 depicts the waveforms applied and the current responses. The nomenclature used was adopted from Helfrick and Bottomley (2009) and kept throughout this work. The cyclic square waveform (CSW) consisted of a square wave oscillation superimposed on a symmetric staircase waveform (Fig. 1A). Note that in this work that CSWs were applied consecutively multiple times resulting in multiple cyclic square wave voltammetry, M-CSWV (Fig. 1B). This exploits the adsorption characteristics of dopamine at CFMs to enable measurements of tonic dopamine concentrations. The waveform parameters, $E_{staircase}$, $E_{Initial}$ ($= E_{End}$) and τ were fixed at 25 mV, −200 mV and 1.0 ms, respectively. $E_{staircase}$ was maintained at 25 mV because it mainly determines the duration of CSW. If the $E_{staircase}$ is too large, the current response is distorted by the potential steps; it should be dominated by E_{SW} and not $E_{staircase}$. $E_{Initial}$ was set to −200 mV to aviod loss of the dopamine redox response to M-CSWV which empirically possess features at −400 mV (see below). The experiment was designed such that the combination of $E_{Initial}$ and E_{SW} caused the potential spanning the redox potential of dopamine to be applied. Lastly, a τ of 1.0 ms was used to give each upward and downward potential sufficient time for the decay of capacitive charging currents to plateau (Fig. 1C). However, τ could not be too long since it also affects the length of CSW.

3.2. M-CSWV of dopamine

The M-CSWV with five CSWs responses to 1.0 μM of dopamine in TRIS buffer shows that this technique can measure tonic dopamine concentrations (Fig. 2). An example of the raw signal recorded from the CFM in a solution of dopamine is shown in Fig. 2A. The signal has two components, a large capacitive charging current and faradaic current due to the dopamine redox reaction at both forward and reverse sweeps. Because the amount of dopamine decreases as successive CSWs are applied, the fifth CSW was subtracted from the second CSW to reveal the difference in the signal. The second CSW was chosen for better selectivity performance as discussed below. Note the result after subtraction is ~100 times smaller than the raw signal. The dopamine redox pattern was still present because the dopamine response to multiple CSWs decays due to the adsorption properties of dopamine to CFM (Bath et al., 2000). However, there was still some non-faradaic components present in the signal due to changes in capacitive charging currents among CSWs. To eliminate this non-faradaic signal, we modelled cyclic square wave voltammograms (CSWV) using the data in Fig. 2A, mimicking a capacitive current difference pattern to minimize the background current difference (Fig. 2B). Typically, voltammetry techniques that apply potential steps generate large capacitive charging currents that rapidly decrease while the potential is held constant (see Fig. 1C) (Osteryoung, 1983). In addition, the large capacitive current decays faster than the current due to the redox reactions (Osteryoung, 1983). To exploit this feature, all current responses generated using M-CSWV were sampled in contrast to conventional pulse wave analyses which sample only at the end of each potential pulse after the capacitive current has decayed. Because all of the current was sampled, the capacitive charging contribution could be modelled and subtracted out. We hypothesized that the capacitive charging current response could be estimated with the exponential decay modelling. The background current for each raw CSWV was thus modelled (Fig. S-2A) using a one phase exponential decay equation ($Y = a \cdot e^{-bx}$, Fig. S-2B). At each upward and downward staircase potential, five points from the peak current were discarded. Then, the next six points and last 20 points were used for modelling with the one phase exponential decay equation (Fig. S-2B). By interpolating data in the middle of the decay curve, the slow redox reactions could be preserved while eliminating fast capacitive current decays. The modelled background current mimicked the

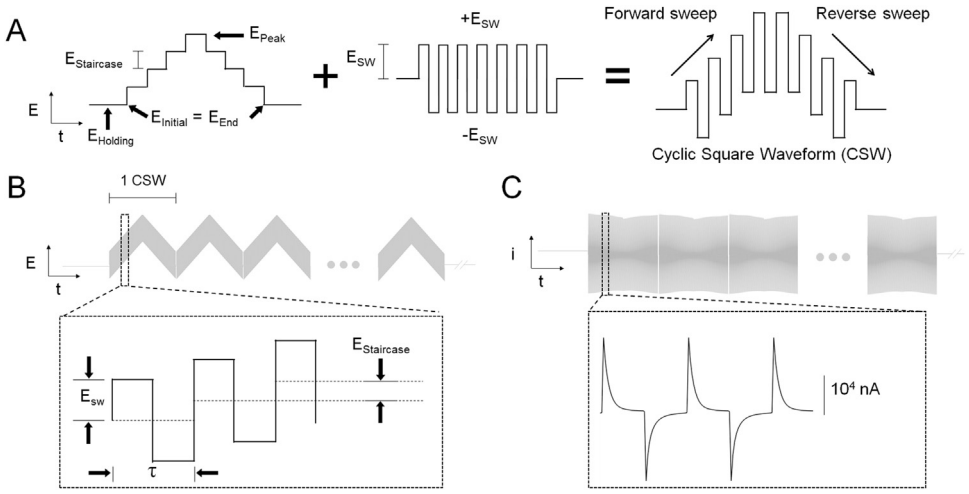

Fig. 1. Schematic design of multiple cyclic square wave voltammetry (M-CSWV). (A) The description of cyclic square waveform (CSW). (B) M-CSWV waveform used in this study. (C) Representative background currents measured by M-CSWV.

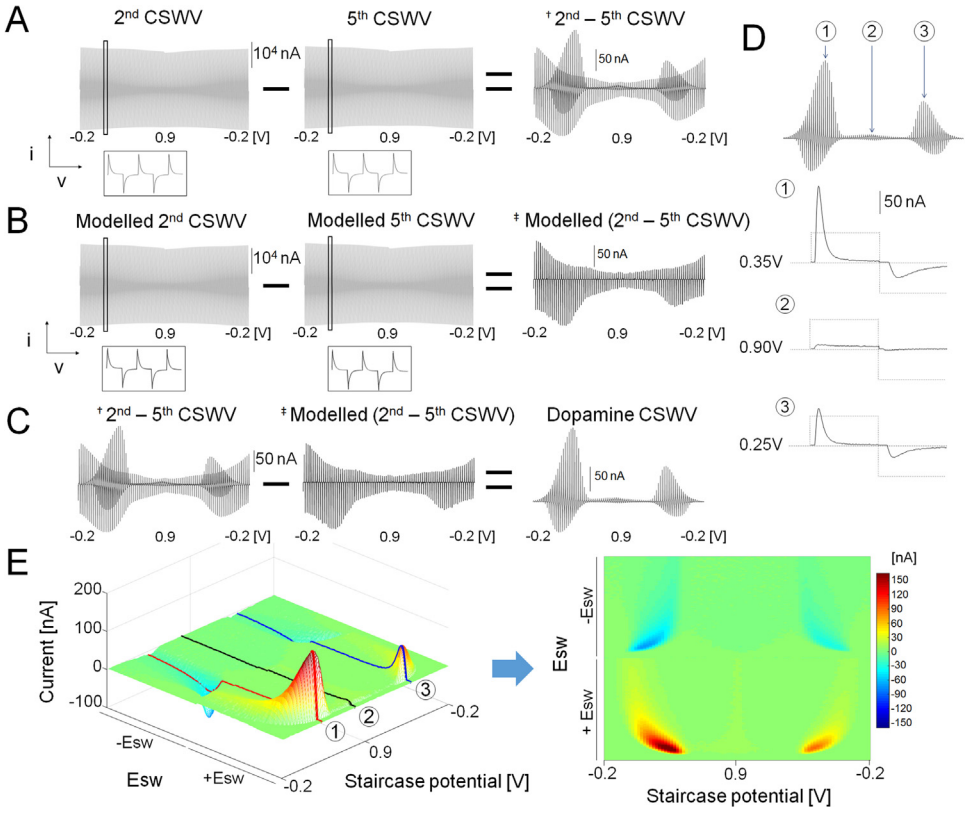

Fig. 2. M-CSWV response for 1 μM dopamine. (A) The background current difference between 2nd and last CSWV. (B) Simulated background current difference between 2nd and last CSWV. (C) Capacitive current removal by subtracting simulated CSWV from raw data. (D) CSWV response for 1 μM of dopamine at different staircase potentials (E) Pseudo color plot of dopamine response to M-CSWV.

difference pattern in Fig. S-2A (Fig. S-2B). Thus, by subtracting the modelled background current from raw signal, the capacitive current in the voltammogram could be minimized (Fig. 2C and S-2C). The dopamine redox response to M-CSWV was subsequently calculated by subtracting the resultant voltammograms from Fig. 2A and B, (Fig. 2C).

The dopamine response to M-CSWV consisted of redox reactions at both forward and reverse sweeps because the square wave modulation covers the redox potential range within a square wave. A maximum dopamine oxidation response occurred at a forward sweep staircase potential of 0.35 V (upward potential: 0.75 V, downward potential: −0.15 V, Fig. 2D-①). The dopamine redox reaction also occurred during the reverse sweep as well at 0.25 V (upward potential: 0.65 V, downward potential: −0.25 V, Fig. 2D-③). As shown in Fig. 2D-②, when the staircase potential did not cover the redox potential, there dopamine redox reactions were absent.

A new plotting method was developed to display the dopamine responses (Fig. 2D) in an effort to provide a better visualization of the data. This involved arranging the square wave responses in the order of the staircase potential (Fig. 2E). The x-axis is the staircase potential, ranging from −200 to 900 mV and back. The staircase potential was modulated with a square wave of ± 400 mV, and this is plotted on the y-axis. The peak current of the redox response was the only information extracted from Fig. 2D. However, dissecting the response into a 2D array enabled a two-dimensional voltammogram (2D voltammogram) to be generated for each scan. The generation of this additional dimension provides important new electrochemical information, such as a two dimensional signature of the redox reaction for each analyte. Thus, 2D voltammograms provide enhanced selectivity to dopamine, compared to conventional FSCV.

3.3. Optimization of M-CSWV parameters to dopamine response

$E_{holding}$, ESW, and the number of waveforms applied were examined in an effort to optimize the dopamine response. When optimizing E_{SW}, the final peak potential (E_{Peak} + E_{SW}) was set at 1.3 V to maximize sensitivity while not causing excessive charging current (Heien et al., 2003). The actual CSW that was used in this process is shown in Fig. S-1. Using CSW from Fig. 1A, multiple CSWs were made with a 2.0 ms gap between each CSW, which is an optimal distance for negligible voltammetric cross talk among waveforms (Fig. 2B) (Jang et al., 2012; Oh et al., 2015). M-CSWV was applied every 10 s to allow sufficient time for dopamine to reach equilibrium between the solution and the CFM surface dopamine concentration (Oh et al., 2016; Atcherley et al., 2013). Both upward/downward potentials generated upward/downward currents as shown in Fig. 1C.

Among the multiple parameters that dictate the M-CSWV waveform, a possible avenue to improve sensitivity was investigated by measuring the dopamine sensitivity as a function of the number of waveforms applied, E_{SW}, and $E_{Holding}$ (Fig. 3). Previous voltammetric techniques utilized a wide range of repetition times (0.1–100 Hz) to generate different dopamine responses within multiple waveforms (Oh et al., 2016; Atcherley et al., 2015). Since the dopamine response difference is directly related to the sensitivity, the number of CSWs used in M-CSWV must be determined. Therefore, M-CSWV composed of 25 CSWs was used to examine the dopamine response using the conventional background subtraction method (*i.e.* we subtracted the signal in buffer from the signal with dopamine present). Responses with 1 μM of dopamine decayed from 400 nA to 100 nA throughout 25 CSWs (Fig. 3A). In Fig. S-3, the representative data showed that dopamine responses decayed until 5th or 6th CSW. Statistically, the first through the fourth waveform showed significant differences when compared to the 25th dopamine signal (Fig. 3A, n = 5 electrodes, $p < 0.0001$, one-way ANOVA test with Dunnett's multiple comparisons, $p < 0.0001$, DF = 24, MS = 24709, F = 41.69). The 5th waveform to the 24th showed no significant difference; therefore, five CSWs were chosen as optimal to minimize the measurement time while maximizing sensitivity.

Next, E_{SW}, the amplitude of square wave, was examined and varied from ± 100 mV to ± 400 mV in 100 mV intervals. The number of waveforms was held constant at five. In the representative data shown in Fig. S-4, the dopamine redox response increased as E_{SW} was made

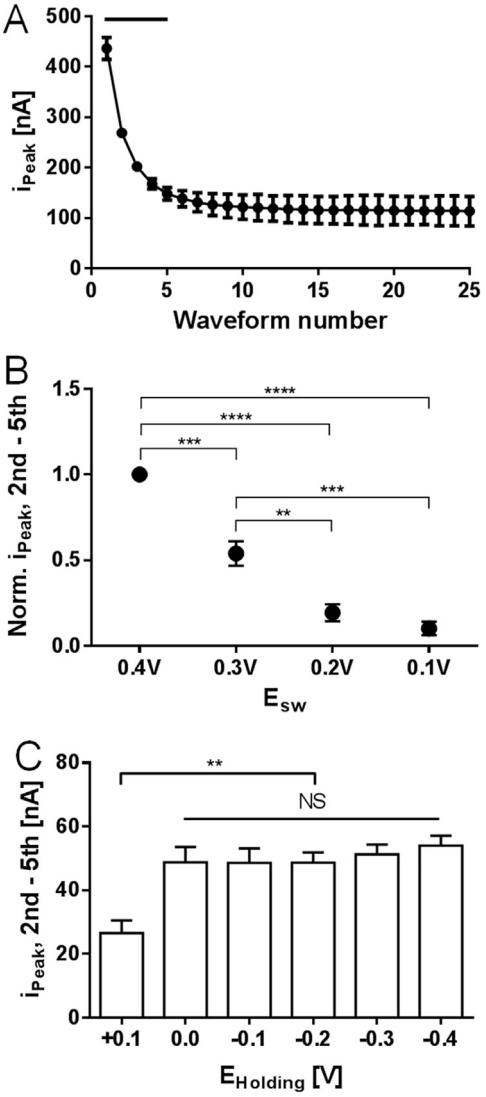

Fig. 3. Parameters for optimal dopamine response of M-CSWV. (A) Dopamine 1 μM response to a number of CSW pulses. Dopamine responses from 1st to 4th waveform showed significant differences from the last voltammogram (Black bar, n = 5 electrodes, $p < 0.0001$, one-way ANOVA test with Dunnett's multiple comparisons). (B) E_{SW} effects on the dopamine response difference between 2nd and 5th M-CSWV. Dopamine responses are normalized. 0.4 V Esw was significantly higher than others (n = 3 electrodes, $p < 0.0001$, one-way ANOVA test with Tukey's multiple comparisons). (C) $E_{Holding}$ effects on the dopamine response difference between 2nd and 5th M-CSWV. Holding potentials from 0 V to − 0.4 V showed no significant difference (n = 5 electrodes, one-way ANOVA test).

larger. Fig. 3B shows the changes in the normalized M-CSWV response (2nd – 5th) to 1.0 μM of dopamine as E_{SW} was varied. An E_{SW} of 400 mV was used for normalizing. The increases in M-CSWV response from E_{SW} 100 to 400 mV can be explained by the larger potential range covered for both oxidation and reduction at each individual square wave. E_{SW} 0.4 V was chosen for M-CSWV because it showed significantly higher sensitivity than other potential steps (n = 3 electrodes, $p < 0.0001$, one-way ANOVA test with Tukey's multiple comparisons, DF = 3, MS = 0.4966, F = 72.78). Potential steps beyond 400 mV were not included in Fig. 3B as they generated too large of a capacitive charging current, making quantification difficult.

To further evaluate the effect of the applied waveform on dopamine sensitivity, the holding potential, $E_{Holding}$, was investigated. Dopamine is positively charged and it is known that the holding potential affects the adsorption of dopamine to CFM (Bath et al., 2000; Takmakov et al., 2010). Therefore, with the holding potential held at a positive potential (0.1 V), the dopamine response was significantly lower than that with negative holding potentials (Fig. 3C, n = 5 electrodes, one-way ANOVA test with Tukey's multiple comparisons, $p < 0.01$, DF = 5, MS = 490.5, F = 6.553). There was no significant difference in i_{peak} values with the $E_{Holding} \leq 0.0$ V as shown in Fig. 3C and S-4. Similar results have been reported previously (Dengler and McCarty, 2013). Therefore, a $E_{Holding}$ potential of 0.0 V was chosen because a lower capacitive charging current has been shown with a 0.0 V holding potential (Oh et al., 2016; Heien et al., 2003).

3.4. Dopamine-kernel to analyse M-CSWV

To develop a method for dopamine quantification, the above optimized parameters were used to collect 2D voltammograms *in vitro* using M-CSWV (Fig. 4A). In this regard, extracting relevant features from the 2D voltammogram is a critical step to quantify the concentration of dopamine. Here, a "dopamine-kernel" was developed and applied to the 2D voltammogram to extract the dopamine features. This approach is similar to the integration method used in Atcherley et al. (2015) To make a dopamine-kernel, the *in vitro* dopamine response of M-CSWV was used and applied to a threshold algorithm where signals greater than 60% of the maximum current in the 2D voltammogram were given a value of one in the dopamine kernel to identify the oxidative features. The remaining points are given a value of zero (Yellow and red, respectively, in Fig. 4B). The dopamine-kernel was then extracted and applied to the 2D voltammogram by element-wise multiplication. This resulted in extracting only the dopamine-feature area from 2D voltammogram, which was then integrated. The integration of the dopamine-feature area corresponded to dopamine concentration (Fig. 4C, Video 1) and the calibration curve followed a quadratic regression (n = 4 electrodes, $R^2 = 0.99$). The accuracy of M-CSWV with the integration method resulted in higher sensitivity (31 pC/μM, with a limit of detection of 0.17 ± 0.03 nM, ± SEM, n = 4 electrodes) as previously reported (Burrell et al., 2015). We attribute this to the fact that the accumulated redox reaction is measured multiple times within a single scan. These results demonstrate that the produced dopamine-kernel improves the estimation of dopamine concentrations from the responses to M-CSWV. Many electrochemical studies use computational methods such as principal component analysis to measure dopamine (Johnson et al., 2016; Heien et al., 2004). In the future, this work can be expanded to make use of the information-rich 2D voltammogram.

Supplementary material related to this article can be found online at doi:10.1016/j.bios.2018.08.034.

3.5. Selectivity for dopamine over electroactive interferents

We tested our method against three common interferents in the rat striatum: two electroactive species, 3,4-dihydroxyphenylacetic acid (DOPAC, 20 μM) and ascorbic acid (AA, 200 μM), and a pH change (Δ − 0.2). DOPAC is a primary metabolic byproduct of dopamine by monoamine oxidase and is thought to be present at 10–20 μM in the extracellular space (Slaney et al., 2012). Ascorbic acid is a major antioxidant in the brain and its concentration is estimated to be in the range of 100–400 μM in the extracellular space (Gonon et al., 1981). Both DOPAC and AA have similar redox potentials to dopamine and relatively much higher extracellular concentrations (Cahill et al., 1996). The M-CSWV response to 20 μM DOPAC is depicted in Fig. 5A. Using conventional background subtraction, we were able to identify each CSWVs response to DOPAC. As a result, the peak currents from 2nd to 5th CSW were not significantly different (Fig. 5A, upper panel, n = 5 electrodes, one-way ANOVA test, Tukey's multiple comparison, $p = 0.71$, SS = 120.0, DF = 9, MS = 13.33, F = 0.69), which means that the dynamic background subtraction between 2nd and 5th can be used to offset DOPAC response to M-CSWV (Fig. 5A, lower panel). The

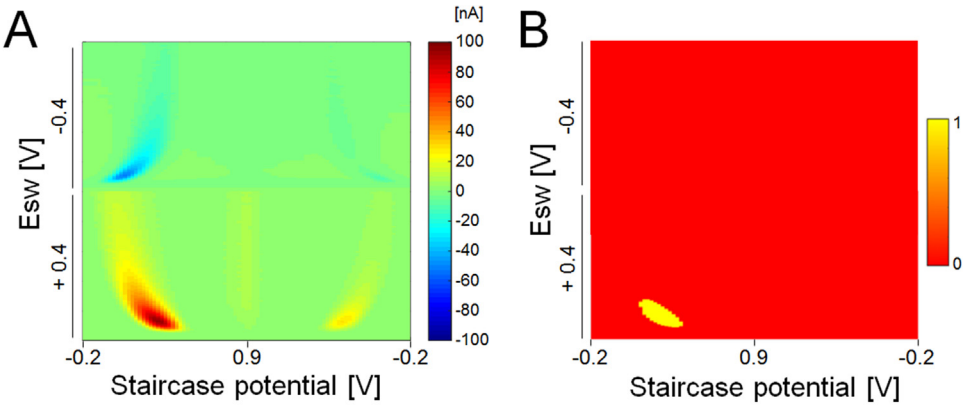

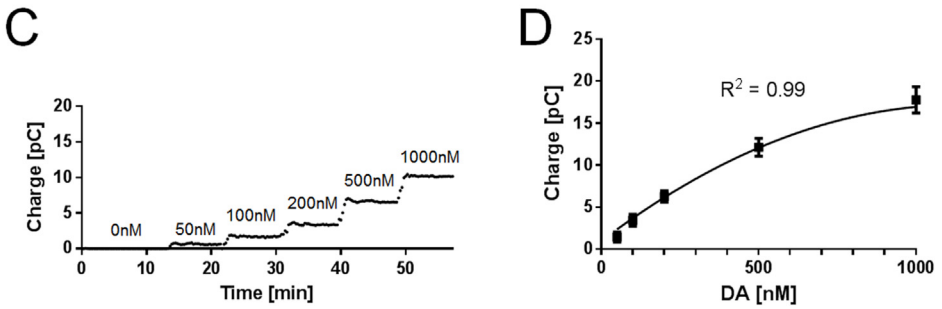

Fig. 4. Dopamine response to M-CSWV and analysis for calibration. (A) Pseudo color plot of 1 μM dopamine response to M-CSWV. (B) Dopamine kernel extracted from (A). Thresholding the pseudo color plot by 60% of the maximum amplitude set the top 40 percentiles (red, dopamine-featured area) to one and remaining (green) to zero. (C) Steady-state current response obtained for the oxidation of dopamine at forward sweep upon the injection of multiple concentrations. (D) A calibration plot obtained by M-CSWV correlates with dopamine concentrations (n = 4 electrodes, R^2 = 0.99, quadratic regression).

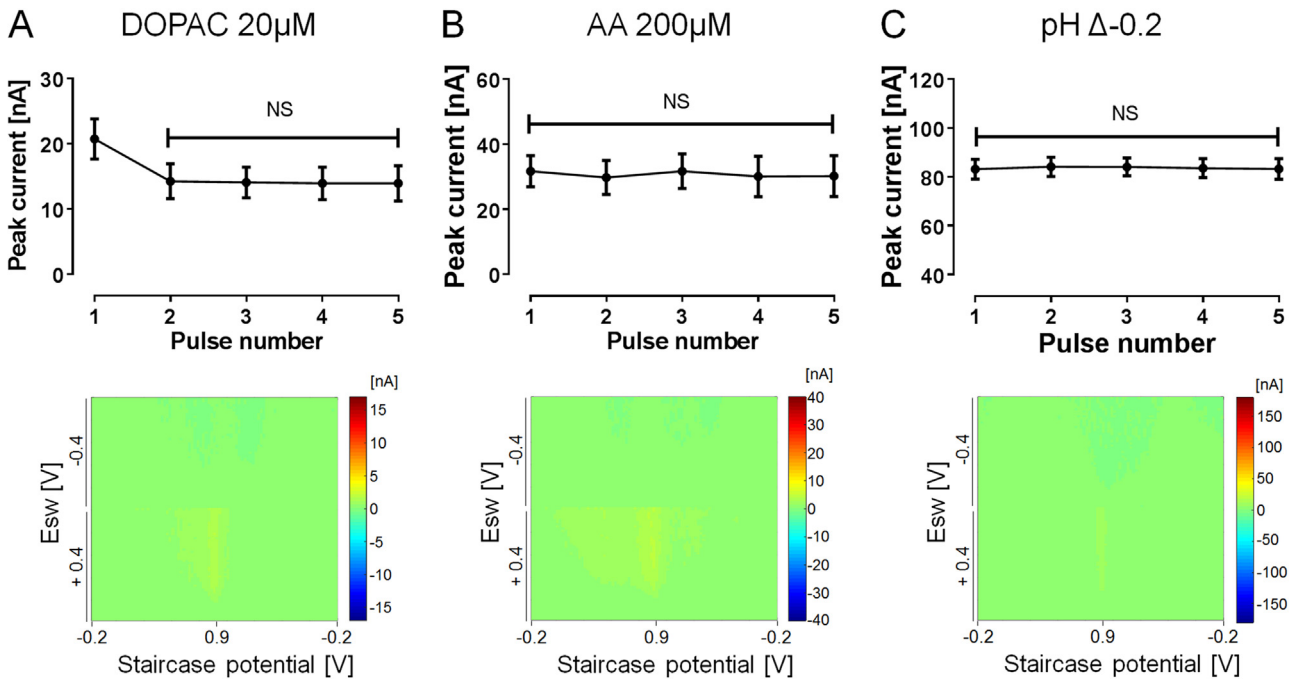

Fig. 5. M-CSWV responses for DOPAC, AA, and pH change. (A) Peak oxidation currents of background-subtracted M-CSWV to DOPAC 20 μM. DOPAC responses from 2nd to 5th CSWV showed no significant differences (n = 5, one-way ANOVA test, upper panel). Pseudo color plot of 20 μM DOPAC response to M-CSWV. DOPAC can be offset by subtracting 2nd and 5th CSWV (lower panel). (B) Peak oxidation currents of background-subtracted M-CSWV to AA 200 μM. AA responses from 2nd to 5th CSWV showed no significant differences (n = 5, one-way ANOVA test, upper panel). Pseudo color plot of 200 μM AA (lower panel). (C) Peak oxidation currents of background-subtracted M-CSWV to pH changes. pH responses from 1st to 5th CSWV showed no significant differences (n = 5, one-way ANOVA test, upper panel). Pseudo color plot of pH changes (lower panel).

representative background-subtracted DOPAC response showed that the 2nd and 5th 2D voltammogram displayed identical redox patterns and the difference between 2nd and 5th response became zero (Fig. S-6A). AA showed similar results with DOPAC, but AA expressed no significant peak currents differences from the 1st CSW (Fig. 5B, upper panel, n = 5 electrodes, one-way ANOVA test, $p > 0.9999$, SS = 12.31, DF = 9, MS = 1.367, F = 0.01423). The M-CSWV response to AA was also offset by subtracting 2nd and 5th (Fig. 5B, lower panel). The representative response of background-subtracted AA is shown in Fig. S-6B. In Fig. S-6B, AA responses in both 2nd and 5th CSW were also identical. These results are consistent with results previously reported (Oh et al., 2016). DOPAC and AA are known for low or non-adsorptive species at CFMs resulting in low sensitivity and fast equilibrium states in multiple pulses (Atcherley et al., 2013). Transient local pH changes

in the brain is an accompanying phenomenon with neuronal activity and it has been a major contributor to capacitive background drift in voltammetry (DeWaele et al., 2017). The features of M-CSWV allow the removal of capacitive charging currents which includes the background drift caused by pH changes. The pH changes showed identical peak currents through all CSWs and the M-CSWV response was also offset (Fig. 5C, n = 5 electrodes, one-way ANOVA test, $p > 0.9999$, SS = 4.269, DF = 9, MS = 0.4743, F = 0.01042). A representative response of background-subtracted pH changes is shown in Fig. S-6C. Other possible electroactive interferents (homovanillic acid, uric acid, and adenosine) were examined *in vitro* to confirm selective measurement of tonic dopamine levels *in vivo*. Homovanillic acid (HVA; 20 μM), uric acid (100 μM), and adenosine (1 μM) resulted in no significant difference in peak current from 1st CSW to 5th CSW, respectively (Fig. S-7, n = 3 electrodes, one-way ANOVA test). These results were expected as these analytes do not significantly adsorb to the carbon fiber surface, compared to dopamine. By adopting a dynamic background subtraction method, enabled confirmation that DOPAC, AA, pH changes, HVA, uric acid, and adenosine do not significantly impact the M-CSWV acquired dopamine response.

3.6. Effect of increased background charging currents on local neuronal activity

Although the currents typically associated with electrochemical measurements performed at microelectrodes (Ø = 7 μM, 50 μM in length) are not enough to affect local neuronal activity (Stamford et al., 1993; Ewing et al., 1983), the charging current generated by M-CSWV is large (> 10 μA, Fig. 1C) when compared to previous voltammetric techniques such as FSCV. To test if the currents generated by the application of M-CSWV would stimulate local neurons, a brain slice Ca^{2+} imaging experiment was performed (Takahashi et al., 1999). A CFM was placed in a mouse striatum slice and the M-CSWV waveform was applied while the Ca^{2+} recordings were made. Eight cells adjacent to the CFM surface were chosen from the microscopic field (Fig. S-8A) and the increases in [Ca^{2+}] were calculated and expressed as ΔF/F (see Supporting Information). The cells responded to KCL aqueous solution introduction and electrical stimulation (200 μA, biphasic, 2 ms pulse width, and 180 pulses). The conventional FSCV waveform (1.3 V peak potential and 400 V/s) did not significantly affect the cell activity as previously reported (Keithley et al., 2011). The M-CSWV waveform also did not significantly affect cell activity (Fig. S8-B). Thus, it is highly unlikely that the M-CSWV generated currents do not affect or stimulate cells adjacent to the CFM despite of its large capacitive charging current.

3.7. Determination of tonic dopamine levels in vivo by M-CSWV

To determine the average baseline "tonic" level of dopamine *in vivo*, M-CSWV was applied every ten seconds to the CFM implanted in the dorsomedial striatum of anesthetized rats for one hour (Fig. 6A). The average baseline dopamine levels were 120 ± 18 nM (n = 7 rats, ± SEM). Tonic extracellular dopamine concentrations measured in rat brain by microdialysis or electrochemical methods are listed in Table S-1. Although these levels are ten-fold higher than those reported in previous microdialysis studies (Gu et al., 2015; Justice, 1993), our data is in accordance other studies that use modified voltammetric techniques to measure tonic dopamine concentrations *in vivo* (Atcherley et al., 2015; Burrell et al., 2015). Microdialysis has been the gold-standard technique to detect tonic extracellular dopamine concentrations because it provides high selectivity given that samples are analysed *ex situ* with chemical separation techniques, such as high performance liquid chromatography and capillary electrophoresis. However, significant limitations imposed by the time required for molecules to equilibrate across the dialysis membrane, the time required to collect sufficient sample size for analysis (temporal resolution of 1–20 min), and most importantly, tissue damage caused by the length and diameter of the dialysis membrane prevent the ability to continuously monitor dopamine levels (Heien and Wightman, 2006). In contrast, M-CSWV offers superior time resolution (a measurement every 10 s) and spatial resolution (7 μm diameter and 50 μm in length) for *in situ* detection of dopamine. These features provide a much lower equilibrium time between the carbon fiber and dopamine molecules for a higher sampling rate.

Pharmacological treatments with different dopaminergic agents designed to modulate tonic dopamine levels were also conducted to confirm M-CSWV selectivity for *in vivo* dopamine detection. As expected, i.p. injection of saline did not alter dopamine tonic levels recorded for 2 h following injection (Fig. 6B, 135 ± 15 nM, n = 5 rats, Video 2). After dopamine is released, it is rapidly cleared from the extracellular space by the dopamine transporter DAT expressed in the pre-synaptic terminals, soma, and dendrites of dopaminergic neurons

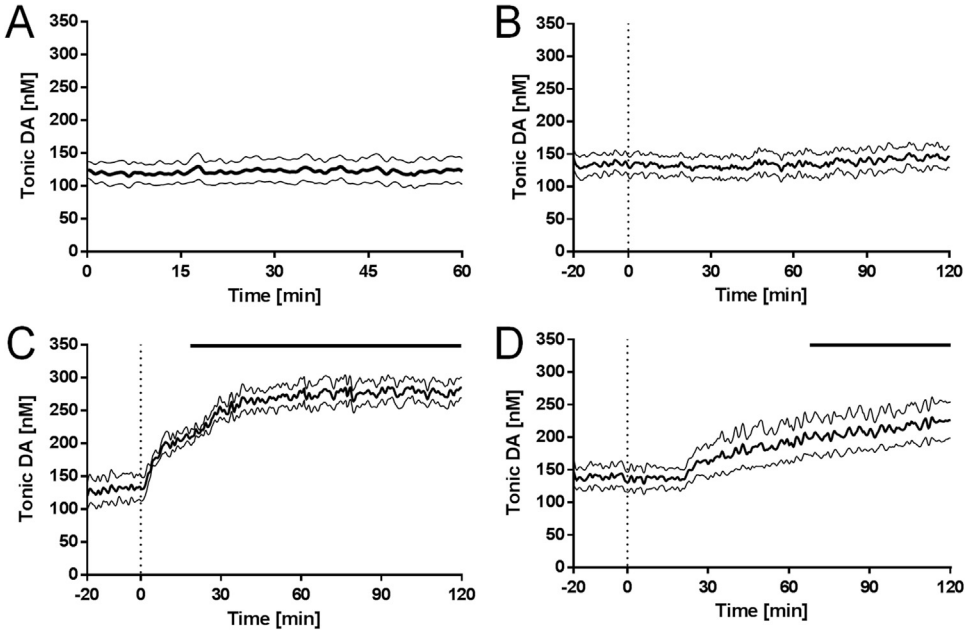

Fig. 6. Pharmacological effects on tonic dopamine concentrations. The tonic dopamine concentrations in response to (A) no treatment controls (n = 7 rats), (B) saline controls (n = 5 rats), (C) nomifensine (n = 5 rats, 20 mg kg-1, i.p.), and (D) pargyline (n = 5 rats, 75 mg kg-1, i.p.). Bold line represents mean concentrations over time, and thin black lines represent the SEM. Bars above at the lower plots indicate significant differences compared to pre-drug injection (n = 5 rats, each group, 2-way ANOVA, $p < 0.0001$, Dunnett's multiple comparisons test).

(Nirenberg et al., 1996). Pharmacological inhibition of DAT with nomifensine or cocaine has been used to show enhanced tonic and phasic levels of dopamine in an activity-dependent manner (Gu et al., 2015; Oh et al., 2016). Systemic administration of the DAT blocker, nomifensine, caused an increase in tonic levels of dopamine that reached a plateau twofold higher than pre-drug baseline levels after 40 min (Fig. 6C, n = 5 rats, Video 3). The average tonic dopamine level elevated from 130 nM to 279 nM after the injection of nomifensine and reached significance ~23 min after the injection (Fig. 6C, upper bar, n = 5 rats, two-way ANOVA, $p < 0.0001$, DF = 4, MS = 22863, F = 17.88).

Supplementary material related to this article can be found online at doi:10.1016/j.bios.2018.08.034

There is a possibility that our tonic measurements are partially due to increased norepinephrine (NE) levels because nomifensine exhibits equal affinity for DAT and the NE transporter (NET). In addition, dopamine can be cleared from the extracellular space by NET in brain regions where dopaminergic projections are relatively low, such as the prefrontal cortex and hippocampus (Sesack et al., 1998). However, NE tissue content in the striatum is negligible and it has been demonstrated that the local infusion of selective NET inhibitors do not affect dopamine levels in the striatum (Carboni et al., 1990).

As well, we determined that the signal was also not due to the electroactive dopamine metabolite DOPAC. After dopamine reuptake, the neurotransmitter is metabolized to DOPAC primarily by MAO, a mitochondrial enzyme that oxides the side chain of dopamine. As shown above (Fig. 5A), M-CSWV was able to cancel out DOPAC by dynamic subtraction. To examine whether the signal originated from DOPAC *in vivo*, the MAO inhibitor pargyline was administered. Inhibition of MAO by pargyline resulted in a delayed and relatively slow increase in striatum tonic levels of dopamine (Fig. 6D, video 4). The rate of dopamine metabolism by MAO is sufficiently slow that it plays little role on the time scale of phasic bursting activity. Hence, no immediate changes have been observed in FSCV recordings of stimulation-evoked dopamine release following MAO inhibition (Heien and Wightman, 2006). However, MAO inhibition significantly increases tonic dopamine, as shown previously (Atcherley et al., 2015; Burrell et al., 2015), because its intraneuronal metabolism competes with its repackaging into vesicles, increasing the availability of dopamine for activity-dependent release. Injection of pargyline elevated the tonic dopamine level from 135 nM to 225 nM for two hours. Because of the slow metabolism, the effects of pargyline on tonic dopamine levels reached significance ~68 min after injection (Fig. 6D, upper bar, n = 5 rats, two-way ANOVA, $p < 0.0001$, DF = 4, MS = 244587, F = 358.5).

Supplementary material related to this article can be found online at doi:10.1016/j.bios.2018.08.034.

4. Conclusions

Measurements of changes in tonic dopamine levels in terminal targets of central dopaminergic neuronal systems has proven critical in advancing our understanding about a range of neurological and psychiatric disorders and in understanding fundamental relationships between neurochemistry, neuropharmacology, and behavior. While FSCV can provide real-time chemical information, the method presently is limited to measuring only phasic changes. Here, we demonstrate the ability of M-CSWV, in combination with CFMs, to quantitatively measure basal tone and drug-induced changes in tonic dopamine extracellular levels. We performed an optimization of the M-CSWV waveform for sensitive and selective dopamine measurements. We utilized the waveform to measure an average tonic dopamine level in rat striatum as 120 ± 18 nM (n = 7 rats) and pharmacologically verified the *in vivo* signal against the most significant electroactive interferents in the striatum. Although the present *in vivo* recordings lasted over 2 h and were able to obtain a pharmacological response, continuous recordings of tonic dopamine levels in chronically implanted awake rats to verify longevity will provide insight into the integrative nature of dopamine systems in the brain. Future research will be focused on maximization of the longevity of electrodes for both anesthetized and awake behaving animal recordings. In this study, M-CSWV was demonstrated as a robust and reliable tool to quantitatively measure tonic dopamine levels which will potentially provide greater insight into dopamine mechanisms in the brain.

Acknowledgement

This research was supported by the NIH 1U01NS090455-01 award and the National Research Foundation of Korea (NRF) grant funded by the Korea government (MSIT) (NRF-2017R1A2B2006896).

Conflict of interest statements

The authors declare no conflict of interest with the studies showed in this article.

Appendix A. Supplementary material

Supplementary data associated with this article can be found in the online version at doi:10.1016/j.bios.2018.08.034.

References

Abdalla, A., Atcherley, C.W., Pathirathna, P., Samaranayake, S., Qiang, B., Pena, E., Morgan, S.L., Heien, M.L., Hashemi, P., 2017. Anal. Chem. 89, 9703–9711.
Atcherley, C.W., Laude, N.D., Parent, K.L., Heien, M.L., 2013. Langmuir: ACS J. Surf. Colloids 29, 14885–14892.
Atcherley, C.W., Wood, K.M., Parent, K.L., Hashemi, P., Heien, M.L., 2015. Chem. Commun. 51, 2235–2238.
Balleine, B.W., Delgado, M.R., Hikosaka, O., 2007. J. Neurosci. 27, 8161–8165.
Bath, B.D., Michael, D.J., Trafton, B.J., Joseph, J.D., Runnels, P.L., Wightman, R.M., 2000. Anal. Chem. 72, 5994–6002.
Burrell, M.H., Atcherley, C.W., Heien, M.L., Lipski, J., 2015. ACS Chem. Neurosci. 6, 1802–1812.
Cahill, P.S., Walker, Q.D., Finnegan, J.M., Mickelson, G.E., Travis, E.R., Wightman, R.M., 1996. Anal. Chem. 68, 3180–3186.
Carboni, E., Tanda, G., Frau, R., Chiara, G.D., 1990. J. Neurochem. 55, 1067–1070.
Dengler, A.K., McCarty, G.S., 2013. J. Electroanal. Chem. 693, 28–33.
DeWaele, M., Oh, Y., Park, C., Kang, Y.M., Shin, H., Blaha, C.D., Bennet, K.E., Kim, I.Y., Lee, K.H., Jang, D.P., 2017. Analyst 142, 4317–4321.
Ewing, A.G., Alloway, K.D., Curtis, S.D., Dayton, M.A., Wightman, R.M., Rebec, G.V., 1983. Brain Res. 261, 101–108.
Floresco, S.B., West, A.R., Ash, B., Moore, H., Grace, A.A., 2003. Nat. Neurosci. 6, 968–973.
Gonon, F., Buda, M., Cespuglio, R., Jouvet, M., 1981. Brain Res. 223, 69–80.
Goto, Y., Otani, S., Grace, A.A., 2007. Neuropharmacology 53, 583–587.
Grace, A.A., 2000. Addiction 95, 119–128.
Grace, A.A., 2016. Nat. Rev. Neurosci. 17, 524.
Grace, A.A., Bunney, B.S., 1984. J. Neurosci. 4, 2877–2890.
Gu, H., Varner, E.L., Groskreutz, S.R., Michael, A.C., Weber, S.G., 2015. Anal. Chem. 87, 6088–6094.
Heien, M., Wightman, R., 2006. CNS Neurol. Disord.-Drug Targets 5, 99–108.
Heien, M.L., Phillips, P.E., Stuber, G.D., Seipel, A.T., Wightman, R.M., 2003. Analyst 128, 1413–1419.
Heien, M.L., Johnson, M.A., Wightman, R.M., 2004. Anal. Chem. 76, 5697–5704.
Heien, M.L., Khan, A.S., Ariansen, J.L., Cheer, J.F., Phillips, P.E., Wassum, K.M., Wightman, R.M., 2005. Proc. Natl. Acad. Sci. USA 102, 10023–10028.
Helfrick Jr, J.C., Bottomley, L.A., 2009. Anal. Chem. 81, 9041–9047.
Howell, J.O., Kuhr, W.G., Ensman, R.E., Wightman, R.M., 1986. J. Electroanal. Chem. Interfacial Electrochem. 209, 77–90.
Huffman, M.L., Venton, B.J., 2009. Analyst 134, 18–24.
Hyman, S.E., Malenka, R.C., 2001. Nat. Rev. Neurosci. 2, 695.
Jang, D.P., Kim, I., Chang, S.-Y., Min, H.-K., Arora, K., Marsh, M.P., Hwang, S.-C., Kimble, C.J., Bennet, K.E., Lee, K.H., 2012. Analyst 137, 1428–1435.
Jay, T.M., 2003. Prog. Neurobiol. 69, 375–390.
Johnson, J.A., Rodeberg, N.T., Wightman, R.M., 2016. ACS Chem. Neurosci. 7, 349–359.
Justice Jr, J., 1993. J. Neurosci. Methods 48, 263–276.
Keithley, R.B., Takmakov, P., Bucher, E.S., Belle, A.M., Owesson-White, C.A., Park, J., Wightman, R.M., 2011. Anal. Chem. 83, 3563–3571.
LeDoux, J., 2012. Neuron 73, 653–676.
Lee, K.H., Lujan, J.L., Trevathan, J.K., Ross, E.K., Bartoletta, J.J., Park, H.O., Paek, S.B., Nicolai, E.N., Lee, J.H., Min, H.-K., 2017. Sci. Rep. 7, 46675.
Nirenberg, M.J., Vaughan, R.A., Uhl, G.R., Kuhar, M.J., Pickel, V.M., 1996. J. Neurosci. 16, 436–447.
Oh, Y., Kim, D.H., Shin, H., Park, C., Chang, S.-Y., Blaha, C.D., Bennet, K.E., Kim, I.Y., Lee,

K.H., Jang, D.P., 2015. Int. J. Electrochem. Sci. 10, 10061–10073.
Oh, Y., Park, C., Kim, D.H., Shin, H., Kang, Y.M., DeWaele, M., Lee, J., Min, H.-K., Blaha, C.D., Bennet, K.E., 2016. Anal. Chem. 88, 10962–10970.
Osteryoung, J., 1983. ACS Publ.
Osteryoung, J.G., Osteryoung, R.A., 1985. Anal. Chem. 57, 101–110.
Robinson, D.L., Venton, B.J., Heien, M.L., Wightman, R.M., 2003. Clin. Chem. 49, 1763–1773.
Schultz, W., 2007. Annu. Rev. Neurosci. 30, 259–288.
Sesack, S.R., Hawrylak, V.A., Matus, C., Guido, M.A., Levey, A.I., 1998. J. Neurosci. 18, 2697–2708.
Slaney, T.R., Mabrouk, O.S., Porter-Stransky, K.A., Aragona, B.J., Kennedy, R.T., 2012. ACS Chem. Neurosci. 4, 321–329.
Stamford, J.A., Palij, P., Davidson, C., Jorm, C.M., Millar, J., 1993. J. Neurosci. Methods 50, 279–290.
Stenken, J.A., 1999. Anal. Chim. Acta 379, 337–358.
Takahashi, A., Camacho, P., Lechleiter, J.D., Herman, B., 1999. Physiol. Rev. 79, 1089–1125.
Takmakov, P., Zachek, M.K., Keithley, R.B., Walsh, P.L., Donley, C., McCarty, G.S., Wightman, R.M., 2010. Anal. Chem. 82, 2020–2028.
Vreeland, R.F., Atcherley, C.W., Russell, W.S., Xie, J.Y., Lu, D., Laude, N.D., Porreca, F., Heien, M.L., 2015. Anal. Chem. 87, 2600–2607.